
PHASE
TRANSITIONS

Processes of Ordering of Structural Elements, Critical and Noncritical Parameters of Phase Transitions in the $(\text{NH}_4)_3\text{WO}_3\text{F}_3$ Crystal

M. S. Molokeev^{a,*} and S. V. Misyul'^{b,**}

^a Kirensky Institute of Physics, Siberian Branch of the Russian Academy of Sciences,
Akademgorodok 50–38, Krasnoyarsk, 660036 Russia

* e-mail: msmolokeev@mail.ru

^b Siberian Federal University, Svobodnyi pr. 79, Krasnoyarsk, 660041 Russia

** e-mail: misjul@kakdem.ru

Received May 5, 2011; in final form, June 28, 2011

Abstract—The structure of the low-temperature triclinic phase of the $(\text{NH}_4)_3\text{WO}_3\text{F}_3$ crystal has been determined and the structure of the cubic phase of this crystal has been refined from data of an X-ray diffraction experiment performed for a powder sample. The profile and structural parameters have been refined according to the procedure implemented in the DDM program. The results obtained have been discussed with invoking the group-theoretical analysis of the complete order parameter condensate, which takes into account the critical and noncritical atomic orderings and allows one to interpret the obtained experimental data. It has been found that the symmetry transformation in the crystal can be schematically represented in the following form: $Fm\bar{3}m$ ($Z = 4$) \longrightarrow $P\bar{1}$ ($Z = 1$) \longrightarrow $P\bar{1}$ ($Z = 6$). This transformation is accompanied by the complete ordering of WO_3F_3 polyhedra and the displacement of NH_4 ions.

DOI: 10.1134/S1063783412010222

1. INTRODUCTION

The main structural elements in compounds of the general formula $A_2BMO_xF_{6-x}$ (where $A, B = \text{K, Rb, Cs}$; $M = \text{Ti, Mo, W}$; $x = 1, 2, 3$) are noncentrosymmetric oxyfluoride anions $\text{MO}_x\text{F}_{6-x}$, which, under specific conditions, allow the formation of polar structures with ferroelectric properties [1]. However, the majority of fluorine–oxygen compounds crystallize in the nonpolar phase of the cubic elpasolite-like structure with a face-centered lattice (space group $Fm\bar{3}m$, $Z = 4$) [1, 2], which, most likely, indicates a fluorine–oxygen disorder in the $\text{MO}_x\text{F}_{6-x}$ anions. With a decrease in the temperature, the majority of the oxyfluorides undergo phase transitions of the ferroelastic or ferroelectric nature due to the processes of ordering and small displacements of atoms [1, 2]. In recent papers [3–6] concerned with the structural investigations of similar compounds, it has been reported that there are problems in explaining the specific features of the structures of both the parent and distorted phases of the aforementioned compounds. This study continues the series of works dedicated to the elucidation of the overall picture of structural transformations occurring during the phase transitions in the crystals under consideration.

The calorimetric investigations performed in our previous work [7] on the $(\text{NH}_4)_3\text{WO}_3\text{F}_3$ crystal

revealed the occurrence of two first-order structural phase transitions at temperatures $T_1 = 200.1 \pm 0.1$ K and $T_2 = 198.5 \pm 0.1$ K with the total change in the entropy $\Delta S_{12} = 18.1 \pm 1.0$ J/(mol K) $\approx R \ln(8.8)$. In [7], it was shown using the X-ray diffraction methods that the $(\text{NH}_4)_3\text{WO}_3\text{F}_3$ crystal exists in the cubic phase G_0 (space group $Fm\bar{3}m$, $Z = 4$) at temperatures above $T_1 = 200.1$ K and undergoes a phase transition to a structure with the pseudotetragonal unit cell at temperatures below T_1 . Vtyurin et al. [8] investigated the variations observed in the Raman scattering spectra of the $(\text{NH}_4)_3\text{WO}_3\text{F}_3$ compound and demonstrated that the phase transitions occurring in this crystal are associated with the orientational ordering of the WO_3F_3 polyhedron. The NH_4 groups play a passive role in the processes of phase transitions and do not undergo ordering.

In order to confirm the above inferences, to specify the order parameters of the phase transitions, and to perform further theoretical descriptions of the structural transformations, it is necessary to determine the structures of distorted low-temperature phases of the compounds under consideration.

Following these objectives, we have carried out more comprehensive temperature X-ray powder diffraction investigations of the structural characteristics

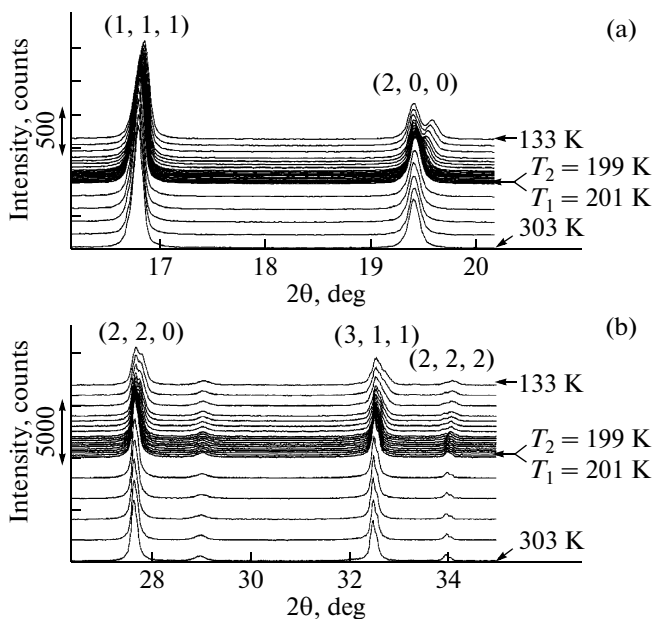


Fig. 1. Fragments of the X-ray diffraction patterns of the $(\text{NH}_4)_3\text{WO}_3\text{F}_3$ compound at different temperatures with the reflections (a) (1, 1, 1) and (2, 0, 0); and (b) (2, 2, 0), (3, 1, 1), and (2, 2, 2). T_1 and T_2 are the temperatures of the phase transitions. $T = 303$ and 133 K are the temperatures at which the structures of the parent and distorted phases were further refined.

and their changes during the phase transitions in the $(\text{NH}_4)_3\text{WO}_3\text{F}_3$ crystal.

2. SAMPLE PREPARATION AND EXPERIMENTAL TECHNIQUE

The synthesis of the studied compound $(\text{NH}_4)_3\text{WO}_3\text{F}_3$ was thoroughly described in [7]. The compound was synthesized from hot solutions of $(\text{NH}_4)_2\text{WO}_2\text{F}_4$ with an excess of NH_4F , followed by gradual addition of an NH_4OH solution up to $\text{pH} = 8$, i.e., up to the formation of first portions of a white precipitate.

The X-ray diffraction patterns from polycrystalline samples of the $(\text{NH}_4)_3\text{WO}_3\text{F}_3$ compound were recorded using an Anton Paar TTK450 temperature chamber installed on a D8-ADVANCE X-ray powder diffractometer (CuK_α radiation, θ - 2θ scan mode, VANTEC linear position-sensitive detector). Liquid nitrogen was used as a coolant. The scan step in the angle 2θ was equal to 0.016° , and exposure per frame was 0.3 s. The experiments were carried out at temperatures in the range from 303 to 133 K with a step varying from 2 to 20 K, depending on how close the temperature of the measurement is to the temperature of the phase transition. This made it possible to reveal regularities in the variations of the structural characteristics of the crystal during the phase transition. In order to more reliably refine the structures of the par-

ent and distorted phases at two temperatures (298 and 133 K), each being fairly different from the phase transition temperature, the exposure at each experimental step was increased to 3 s.

3. EXPERIMENTAL RESULTS

By applying the homology method [9] to analyzing the splittings of X-ray reflections from the parent cubic phase in the X-ray diffraction pattern with a decrease in the temperature (Figs. 1a and 1b), it can be affirmed that symmetry of the distorted phase is either orthorhombic, or monoclinic, or triclinic.

The changes in the translational symmetry in the course of phase transitions occurring in the $(\text{NH}_4)_3\text{WO}_3\text{F}_3$ compound were difficult to reveal in the X-ray diffraction patterns because of the presence of a small number of weak reflections both from impurities and from the ice phase. However, in the angle ranges $2\theta \sim 21.6^\circ$ and $2\theta \sim 37^\circ$ at temperatures below 199 K, we revealed the superstructure reflections (0, 1, 2), (0, $1/3$, $11/3$), (3, $1/3$, $7/3$), and (1, $1/3$, $11/3$) (the indices are given in terms of the parameters of the cubic unit cell). These angle ranges were thoroughly scanned in such a way that the temperature of the sample was varied in the range from 203 to 143 K (Fig. 2) and the exposure at each new temperature was increased to 10 min. This made it possible to elucidate the temperature behavior of the integrated intensity of the aforementioned superstructure reflections (Fig. 3). For processing the X-ray diffraction patterns and determining the integrated intensities of the X-ray reflections from these diffraction patterns, we used the EVA program, which is implemented in the DIFFRAC-PLUS software package (Bruker).

A linear increase in the integrated intensities of superstructure reflections with a decrease in the temperature beginning from $T_1 = 201$ K suggests that the dominant contribution to their intensities are made by the critical order parameters. At the same time, the appearance of the reflections (0, $1/3$, $11/3$), (0, $1/3$, $7/3$), and (1, $1/3$, $11/3$) from the distorted phase at temperatures below 201 K indicates a change in the unit cell volume of the crystal during the phase transition. An attempt to determine the parameters of the triclinic unit cell of the G_2 phase with the known program ITO [10] has failed for a number of reasons, which will be analyzed in a forthcoming publication. In this paper, we have described an original program that makes it possible to properly choose the parameters of the distorted unit cells in accordance with the splitting of the principal reflections and from the comparison of the positions of the superstructure reflections in the X-ray diffraction pattern with the theoretically calculated positions of these reflections. In the nearest future, it is planned to publish an article devoted to a detailed description of this program. The writing such a program is not accidental, because the

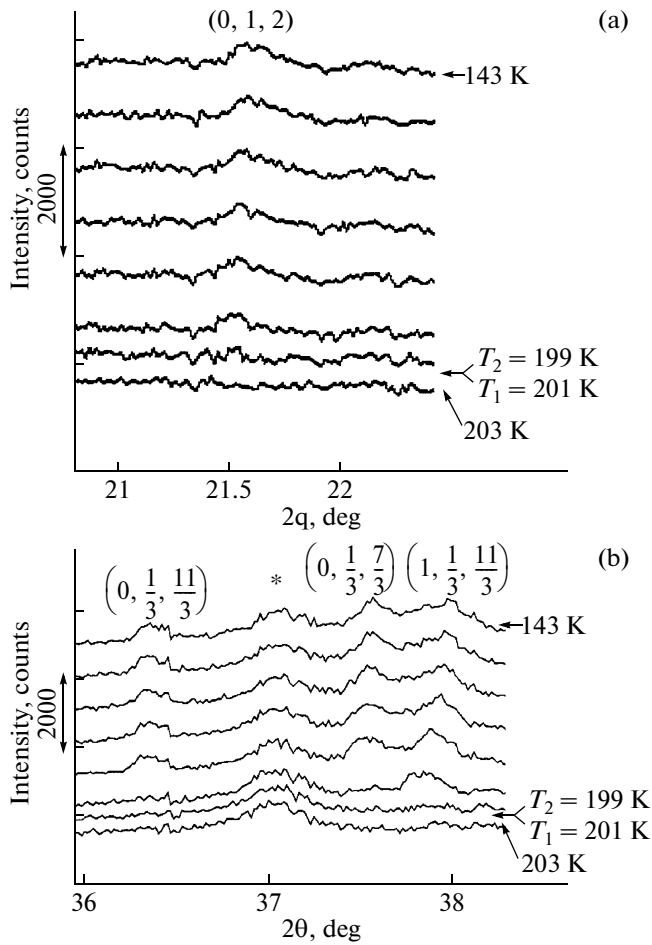


Fig. 2. Fragments of the X-ray diffraction patterns of the $(\text{NH}_4)_3\text{WO}_3\text{F}_3$ compound measured with variations in the temperature in the region of superstructure reflections: (a) $(0, 1, 2)$ and (b) $(0, 1/3, 11/3)$, $(0, 1/3, 7/3)$, and $(1, 1/3, 11/3)$. The asterisk indicates the peak of the impurity. T_1 and T_2 are the temperatures of phase transitions.

above-described task could not be solved by the program ITO [10].

By using the homology method [9] and the original program for the determination of the point and translational symmetries of the distorted phase with decreasing temperature, it has been established that only the triclinic unit cell with $V_i/V_0 = 6$ and the parameters $\mathbf{a}_1 = (\mathbf{a}_0 - \mathbf{b}_0)/2$, $\mathbf{b}_1 = \mathbf{c}_0$, and $\mathbf{c}_1 = -(\mathbf{a}_0 + \mathbf{b}_0)3/2$ is suitable for the description of the entire profile of the X-ray diffraction pattern of the distorted phase, including the splittings of the principal reflections (Figs. 1a and 1b) and the superstructure reflections.

The structural model of the distorted phase was determined using the traditional Patterson function method. The profile and structural parameters were refined according to the procedure implemented in the DDM program [11] (Table 1). The shapes of the

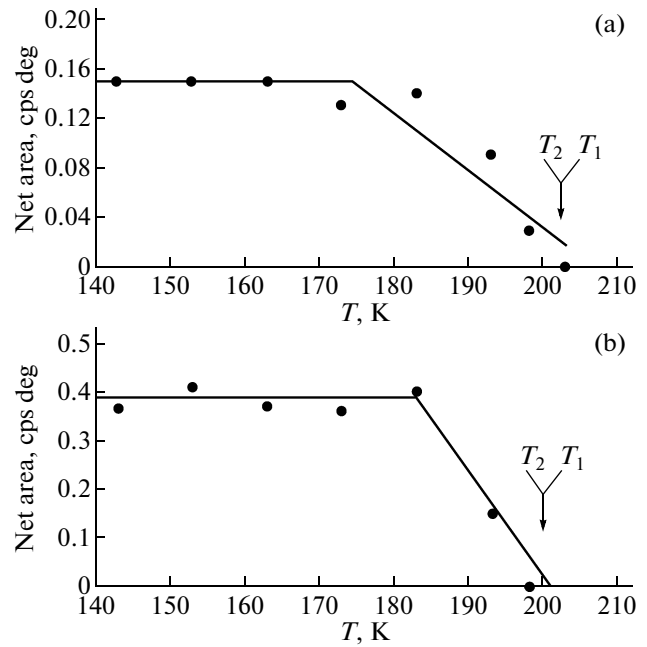


Fig. 3. Temperature dependences of the total integrated intensity of superstructure reflections from the $(\text{NH}_4)_3\text{WO}_3\text{F}_3$ compound: (a) $(0, 1, 2)$ and (b) $(0, 1/3, 11/3)$, $(0, 1/3, 7/3)$, and $(1, 1/3, 11/3)$.

peaks were described by the Pearson VII function. Figures 4a and 4b illustrate the thermal behavior of the parameters of the reduced cubic unit cell, which were obtained during the fitting of the profiles of the X-ray diffraction patterns with the DDM program. It should be noted that, with a decrease in the temperature, the volume of the cubic unit cell increases abruptly by approximately 0.05% at the temperature of the phase transition (see Fig. 4c), which is possible in first-order phase transitions.

In the high-temperature cubic phase G_0 at a temperature of 293 K, the $(\text{NH}_4)_3\text{WO}_3\text{F}_3$ crystal has a cubic cryolite structure. The primitive cell contains one tungsten ion and two independent ammonium ions NH_4 , while the fluorine and oxygen ions are disordered over the position $96k$ with the occupation multiplicity of the position of $1/8$. The thermal parameter of the fluorine and oxygen ions was refined in the isotropic approximation. This model of the disordering of the fluorine and oxygen ions in the cubic phase leads to the minimum discrepancy factor and has been confirmed by the structure of the distorted phase G_2 . Among the two independent ammonium ions, one ion (located in the position $4b$) in the cubic phase has been disordered at least over two positions, which has made it impossible to determine the coordinates of its hydrogen atoms. The other ammonium ion (located in the position $8c$) has already been ordered in the cubic phase, and its atoms have been located (Table 2).

Table 1. Data collection and structure refinement parameters of the $(\text{NH}_4)_3\text{WO}_3\text{F}_3$ compound

Parameter	$T = 298 \text{ K}$	$T = 133 \text{ K}$
Space group	$Fm\bar{3}m$	$P\bar{1}$
$\mathbf{a}_i, \text{Å}$	$\mathbf{a}_0, 9.1531(1)$	$(\mathbf{a}_0 - \mathbf{b}_0)/2, 6.4538(5)$
$\mathbf{b}_i, \text{Å}$	$\mathbf{b}_0, 9.1531(1)$	$\mathbf{c}_0, 9.1507(4)$
$\mathbf{c}_i, \text{Å}$	$\mathbf{c}_0, 9.1531(1)$	$-(\mathbf{a}_0 + \mathbf{b}_0)3/2, 19.2771(7)$
α, deg	90	90.092(3)
β, deg	90	90.509(3)
γ, deg	90	90.231(5)
$V, \text{Å}^3$	766.85(2)	1138.4(1)
Z	4	6
2θ angle range, deg	5–110	5–110
Number of reflections	40	2850
Number of parameters refined	9	101
$R_B, \%$	4.8	6.04
$R_{\text{DDM}}, \%$	13.12	12.79

Note: R_B is the Bragg integral discrepancy factor, and R_{DDM} is the profile discrepancy factor determined with the DDM program [11].

Unfortunately, our attempts to determine the structure of the intermediate phase G_1 have failed because of the narrow temperature region of its existence ($T_2 - T_1 \approx 2 \text{ K}$) and the influence of the transition effects in this region.

The search for the structural model of the other lower temperature triclinic phase G_2 at a temperature of 133 K was performed by analogy with the search for the structure of the cubic phase G_0 at a temperature of 298 K. The primitive cell of the triclinic phase G_2 of the $(\text{NH}_4)_3\text{WO}_3\text{F}_3$ compound contains three tungsten ions and nine independent ions NH_4 . In the triclinic phase G_2 , we also could not determine the coordinates of the hydrogen atoms of the ammonium groups, which have been disordered in the cubic phase G_0 . Therefore, we can state that this ammonium ion remains disordered also in the triclinic phase G_2 . Moreover, we have determined the positions of the hydrogen atoms of the other ammonium groups, which have already been disordered in the cubic phase (Table 2).

The refinement of the proposed structural models of the cubic and triclinic phases of the $(\text{NH}_4)_3\text{WO}_3\text{F}_3$ compound was stable and led to low discrepancy factors. The results of the structure refinement are presented in Tables 1 and 2. The selected bond lengths in the structure of the $(\text{NH}_4)_3\text{WO}_3\text{F}_3$ compound are listed in Table 3. The structures of the cubic phase G_0 and the triclinic phase G_2 of the $(\text{NH}_4)_3\text{WO}_3\text{F}_3$ compound are shown in Fig. 5.

All the WO_3F_3 ions involved in the G_2 phase form hydrogen bonds with the ammonium ions (Fig. 6). In turn, this leads to the formation of a three-dimensional framework, so that each WO_3F_3 polyhedron is

bonded to the neighboring polyhedra through the ammonium ions by the hydrogen bonds.

4. DISCUSSION OF THE RESULTS

The further consideration of the experimental data will be performed according to the scheme used in our recent publications [3, 6], which is based on the works dealing with the group-theoretical analysis of the structural phase transitions in crystals with the space group $Fm\bar{3}m$ [12] and on the ISOTROPY [13] and ISODISPLACE [14] software packages.

At the first stage of our consideration, we determined the order parameters and the representations of the space group $Fm\bar{3}m$, which are involved in the phase transitions. For this purpose, we analyzed the permutation and mechanical representations [15] of the structures of the phases in the $(\text{NH}_4)_3\text{WO}_3\text{F}_3$ crystal. This analysis was carried out with the ISODISPLACE software package [14]. So, using the known structures of the cubic phase G_0 and the triclinic phase G_2 , we performed the expansion of the orderings and displacements of the atoms involved in the $(\text{NH}_4)_3\text{WO}_3\text{F}_3$ crystal, which are transformed according to the irreducible representations of the space group $Fm\bar{3}m$. According to this analysis, the largest contributions to the distortion of the structure are made by the following three representations: Γ_5^+ (11–7) with the order parameter (η_1, η_2, η_3) , $\Sigma_1(4-1)$ with the order parameter $(\xi, 0, 0, -\xi/\sqrt{3}, 0, 0, 0, 0, 0, 0, 0)$, and $\Sigma_3(4-3)$ with the order parameter $(\epsilon, 0, 0,$

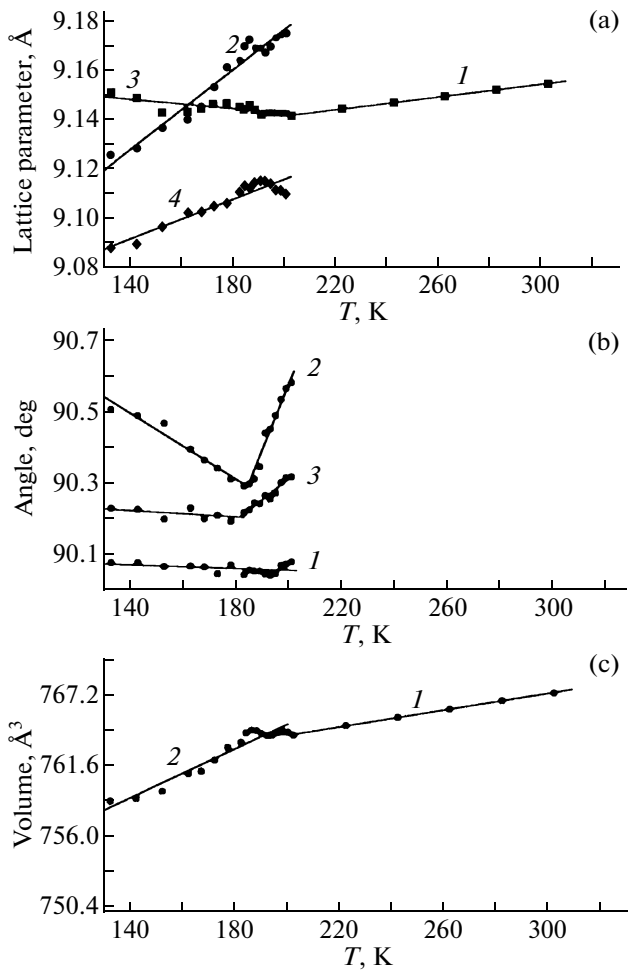


Fig. 4. Temperature dependences of the structural characteristics of the $(\text{NH}_4)_3\text{WO}_3\text{F}_3$ compound. (a) (1) The unit cell parameter a_0 of the cubic phase G_0 and (2–4) the unit cell parameters of the triclinic phase G_2 : (2) $a_1/\sqrt{2}$, (3) b_1 , and (4) $3c_1/\sqrt{2}$; (b) the unit cell angles of the triclinic phase G_2 : (1) α_1 , (2) β_1 , and (3) γ_1 ; and (c) the unit cell volumes of (1) the cubic phase G_0 and (2) the triclinic phase G_2 .

$\varepsilon\sqrt{3}, 0, 0, 0, 0, 0, 0, 0, 0$). The parentetic designations referring to the irreducible representations and the points of the Brillouin zone are given in accordance with the reference book [16]. The appearance of the aforementioned order parameters in the triclinic phase G_2 leads to an ordering of the WO_3F_3 polyhedra and atomic displacements in the structure of the $(\text{NH}_4)_3\text{WO}_3\text{F}_3$ compound.

Thus, the changes in the point and translational symmetry, which are indicated by the positions of the superstructure reflections of the G_2 phase in the X-ray diffraction patterns, can be described by the interaction of three phenomenological order parameters so that one of these order parameters is transformed

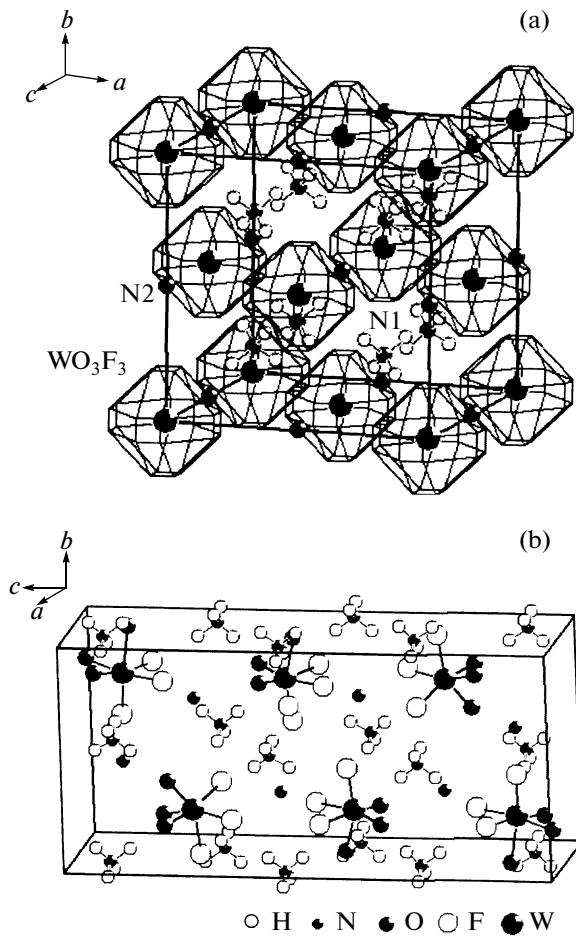


Fig. 5. Structures of the phases of the $(\text{NH}_4)_3\text{WO}_3\text{F}_3$ compound: (a) the cubic phase G_0 at a temperature $T = 298$ K and (b) the triclinic G_2 at a temperature $T = 133$ K.

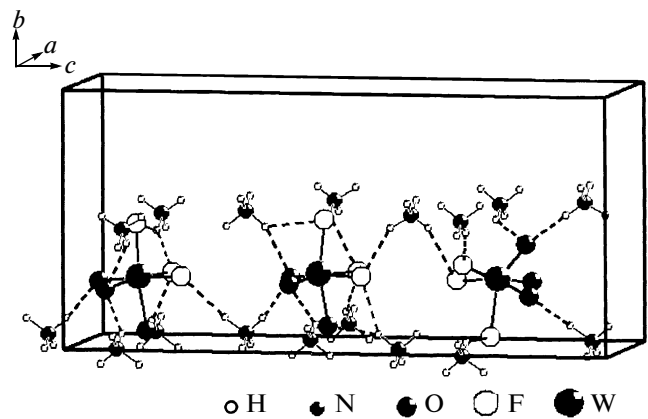


Fig. 6. System of hydrogen bonds in the structure of the $(\text{NH}_4)_3\text{WO}_3\text{F}_3$ compound in the triclinic phase G_2 .

Table 2. Atomic coordinates, isotropic thermal parameters (B_{iso}), and position occupancies (p) in the $(\text{NH}_4)_3\text{WO}_3\text{F}_3$ structure

Atom	p	X	Y	Z	$B_{\text{iso}}, \text{\AA}^2$	Atom	p	X	Y	Z	$B_{\text{iso}}, \text{\AA}^2$
$T = 298 \text{ K}, Fm\bar{3}m$						N13	1.0	0.74(3)	0.74(3)	0.74(1)	2.0
W	1.0	0	0	0	3.02(3)	N21	1.0	0.75(3)	0.01(2)	0.92(1)	2.0
N1	1.0	1/4	1/4	1/4	5.5(3)	H11	1.0	0.75(3)	0.07(2)	0.88(1)	2.0
H1	1.0	0.19	0.19	0.19	4	H12	1.0	0.75(3)	0.07(2)	0.95(1)	2.0
N2	1.0	1/2	1/2	1/2	5.1(4)	H13	1.0	0.64(3)	0.96(2)	0.92(1)	2.0
O	1/8	0.1965(6)	0.0444(4)	0.0444(4)	2.6(2)	H14	1.0	0.86(3)	0.96(2)	0.92(1)	2.0
F	1/8	0.1965(6)	0.0444(4)	0.0444(4)	2.6(2)	N22	1.0	0.78(2)	0.02(2)	0.276(9)	2.0
$T = 133 \text{ K}, P\bar{1}$						H21	1.0	0.78(2)	0.08(2)	0.240(9)	2.0
W1	1.0	0.742(4)	0.246(3)	0.748(1)	3.26(4)	H22	1.0	0.78(2)	0.08(2)	0.312(9)	2.0
F11	1.0	0.54(2)	0.68(2)	0.294(7)	2.0	H23	1.0	0.67(2)	0.97(2)	0.276(9)	2.0
F12	1.0	0.10(2)	0.77(1)	0.339(9)	2.0	H24	1.0	0.89(2)	0.97(2)	0.276(9)	2.0
F13	1.0	0.37(2)	0.97(2)	0.258(9)	2.0	N23	1.0	0.70(2)	-0.03(2)	0.567(8)	2.0
O14	1.0	0.44(2)	0.81(2)	0.18(1)	2.0	H31	1.0	0.70(2)	0.03(2)	0.530(8)	2.0
O15	1.0	-0.01(2)	0.78(2)	0.208(9)	2.0	H32	1.0	0.70(2)	0.03(2)	0.602(8)	2.0
O16	1.0	0.20(2)	0.62(1)	0.204(7)	2.0	H33	1.0	0.59(2)	0.92(2)	0.567(8)	2.0
W2	1.0	0.739(5)	0.240(3)	0.085(1)	1.8(5)	H34	1.0	0.80(2)	0.92(2)	0.566(8)	2.0
F21	1.0	0.18(2)	0.56(2)	0.924(9)	2.0	N24	1.0	0.26(2)	0.44(2)	0.091(9)	2.0
F22	1.0	0.40(2)	0.75(2)	0.826(7)	2.0	H41	1.0	0.26(2)	0.50(2)	0.054(9)	2.0
F23	1.0	0.99(3)	0.76(2)	0.872(8)	2.0	H42	1.0	0.26(2)	0.50(2)	0.126(9)	2.0
O24	1.0	0.51(2)	0.80(2)	0.959(9)	2.0	H43	1.0	0.15(2)	0.39(2)	0.090(9)	2.0
O25	1.0	0.10(3)	0.79(2)	0.00(1)	2.0	H44	1.0	0.37(2)	0.39(2)	0.090(9)	2.0
O26	1.0	0.30(3)	0.97(2)	0.903(9)	2.0	N25	1.0	0.25(3)	0.51(2)	0.41(1)	2.0
W3	1.0	0.758(2)	0.258(2)	0.4147(9)	1.0(4)	H51	1.0	0.25(3)	0.56(2)	0.38(1)	2.0
F31	1.0	0.07(2)	0.24(1)	0.466(7)	2.0	H52	1.0	0.25(3)	0.56(2)	0.45(1)	2.0
F32	1.0	0.60(2)	0.26(1)	0.506(9)	2.0	H53	1.0	0.14(3)	0.46(2)	0.41(1)	2.0
F33	1.0	0.86(2)	0.46(2)	0.421(9)	2.0	H54	1.0	0.36(3)	0.46(2)	0.41(1)	2.0
O34	1.0	0.48(3)	0.23(2)	0.38(1)	2.0	N26	1.0	0.12(2)	0.51(2)	0.727(2)	2.0
O35	1.0	0.67(3)	0.06(2)	0.44(1)	2.0	H61	1.0	0.12(2)	0.57(2)	0.691(7)	2.0
O36	1.0	0.95(2)	0.23(2)	0.35(1)	2.0	H62	1.0	0.12(2)	0.57(2)	0.763(7)	2.0
N11	1.0	0.82(2)	0.65(1)	0.075(8)	2.0	H63	1.0	0.02(2)	0.46(2)	0.727(7)	2.0
N12	1.0	0.73(3)	0.76(2)	0.40(1)	2.0	H64	1.0	0.23(2)	0.46(2)	0.727(7)	2.0

according to the irreducible representation of the space group $Fm\bar{3}m$ with the wave vector Γ at the center of the Brillouin zone (the wave vector $\mathbf{k}_{11} = (0, 0, 0)$) and the other two order parameters are transformed according to the representation with the wave vector Σ at the point located inside the Brillouin zone (the wave vector $\mathbf{k}_4 = (1/3, 1/3, 0)$). These order parameters, which specify the symmetry of the distorted phase, are referred to, in accordance with [17], as the critical order parameters. The structural distortions, atomic displacements, and atomic orderings, which are related to the critical order parameter, are also referred to as critical.

For the further consideration of the mechanism responsible for the phase transitions, we will simulate the ordering of the WO_3F_3 octahedron, which, according to the data reported in [8, 18], has the symmetry corresponding to $3mm(C_{3v})$. The simulation will be performed by analogy with the procedure used in our recent works [3, 6]. In the aforementioned works, such polyhedron was represented as a vector directed from the geometric center of the triangle formed by the oxygen atoms to the center of the triangle formed by the fluorine atoms. In the cubic unit cell, the WO_3F_3 octahedron is oriented in such a way that this vector has the coordinates (x, x, x) ; i.e., it is in the position $32f$ of the face-centered cubic unit cell. By replacing the octahedron with the vector, it is easy to obtain the number of

Table 3. Lengths of the W–F and W–O bonds in the $(\text{NH}_4)_3\text{WO}_3\text{F}_3$ structure at a temperature of 133 K

Bond	Length, Å	Bond	Length, Å	Bond	Length, Å
W1–F11	2.1(1)	W2–F21	1.9(1)	W3–F31	2.2(1)
W1–F12	2.0(2)	W2–F22	2.0(1)	W3–F32	2.0(2)
W1–F13	2.1(2)	W2–F23	2.0(1)	W3–F33	1.9(2)
W1–O14	1.9(2)	W2–O24	1.8(1)	W3–O34	1.9(2)
W1–O15	1.9(2)	W2–O25	1.9(2)	W3–O35	1.9(2)
W1–O16	1.6(1)	W2–O26	1.9(2)	W3–O36	1.8(2)

Note: At a temperature of 298 K, the W–F and W–O bond lengths in the cubic phase are equal to 1.888(5) Å.

Table 4. Symmetries of the $(\text{NH}_4)_3\text{WO}_3\text{F}_3$ phases and relationships between the phenomenological order parameters and the entropies of the phase transitions

Characteristic	$T > 201$ K	$201 > T > 199$ K	$T < 199$ K
Critical representations and order parameters	–	$\Gamma_5^+(11-7)$ (η_1, η_2, η_3)	$\Gamma_5^+(11-7)$ (η_1, η_2, η_3) + $\Sigma_1(4-1)$ ($\xi, 0, 0, -\xi/\sqrt{3}, 0, 0, 0, 0, 0, 0, 0$) + $\Sigma_3(4-3)$ ($\varepsilon, 0, 0, \varepsilon/\sqrt{3}, 0, 0, 0, 0, 0, 0, 0$)
Space group	$Fm\bar{3}m$	$P\bar{1}$	$P\bar{1}$
\mathbf{a}_i	\mathbf{a}_0	$(\mathbf{b}_0 + \mathbf{c}_0)/2$	$(\mathbf{a}_0 - \mathbf{b}_0)/2$
\mathbf{b}_i	\mathbf{b}_0	$(\mathbf{a}_0 + \mathbf{c}_0)/2$	c_0
\mathbf{c}_i	\mathbf{c}_0	$(\mathbf{a}_0 + \mathbf{b}_0)/2$	$-(\mathbf{a}_0 + \mathbf{b}_0)3/2$
Z_i	4	1	6
Experimental entropies	–		$R\ln 8.8$
Calculated entropies	–	$R\ln 4$	$R\ln 2$

different orientations of the WO_3F_3 octahedron in the cubic phase. Since the (x, x, x) position in the cubic phase has a multiplicity of 32, the number of orientations of the WO_3F_3 octahedron in a particular site is $N_0 = 32/Z = 8$, where $Z = 4$ is the number of formula units in the face-centered cubic unit cell. Thus, in the cubic phase, there are eight differently oriented WO_3F_3 octahedra or the vectors replacing the WO_3F_3 group (Fig. 7).

The group-theoretical analysis of the permutation representation makes it possible to easily determine how the occupancies of these eight positions change with variations in the symmetry and, consequently, to elucidate which of the orientations of the octahedron can occur with a higher probability or can be energetically more favorable after the phase transition when the critical order parameter is known. For these purposes, it is most convenient to use the ISODISPLACE

software package [14], because it visualizes the obtained result.

Using the available experimental data [7], we will attempt to determine the sequence of the appearance of order parameters during the phase transitions. Earlier, it was mentioned that the calorimetric investigations carried out in [7] on the $(\text{NH}_4)_3\text{WO}_3\text{F}_3$ crystal revealed the existence of two first-order structural phase transitions at temperatures $T_1 = 200.1 \pm 0.1$ K and $T_2 = 198.5 \pm 0.1$ K with the total change in the entropy $\Delta S_{12} = 18.1 \pm 1.0$ J/(mol K) $\approx R\ln(8.8)$. In this case, judging from the curve reflecting the thermal behavior of the heat capacity [7], the first phase transition at the temperature T_1 makes the greatest contribution to the entropy of the phase transition. By considering the ordering of the WO_3F_3 ion, which is related to the order parameter of only the representation Γ_5^+ (Figs. 7 and 8), it is easy to find that the

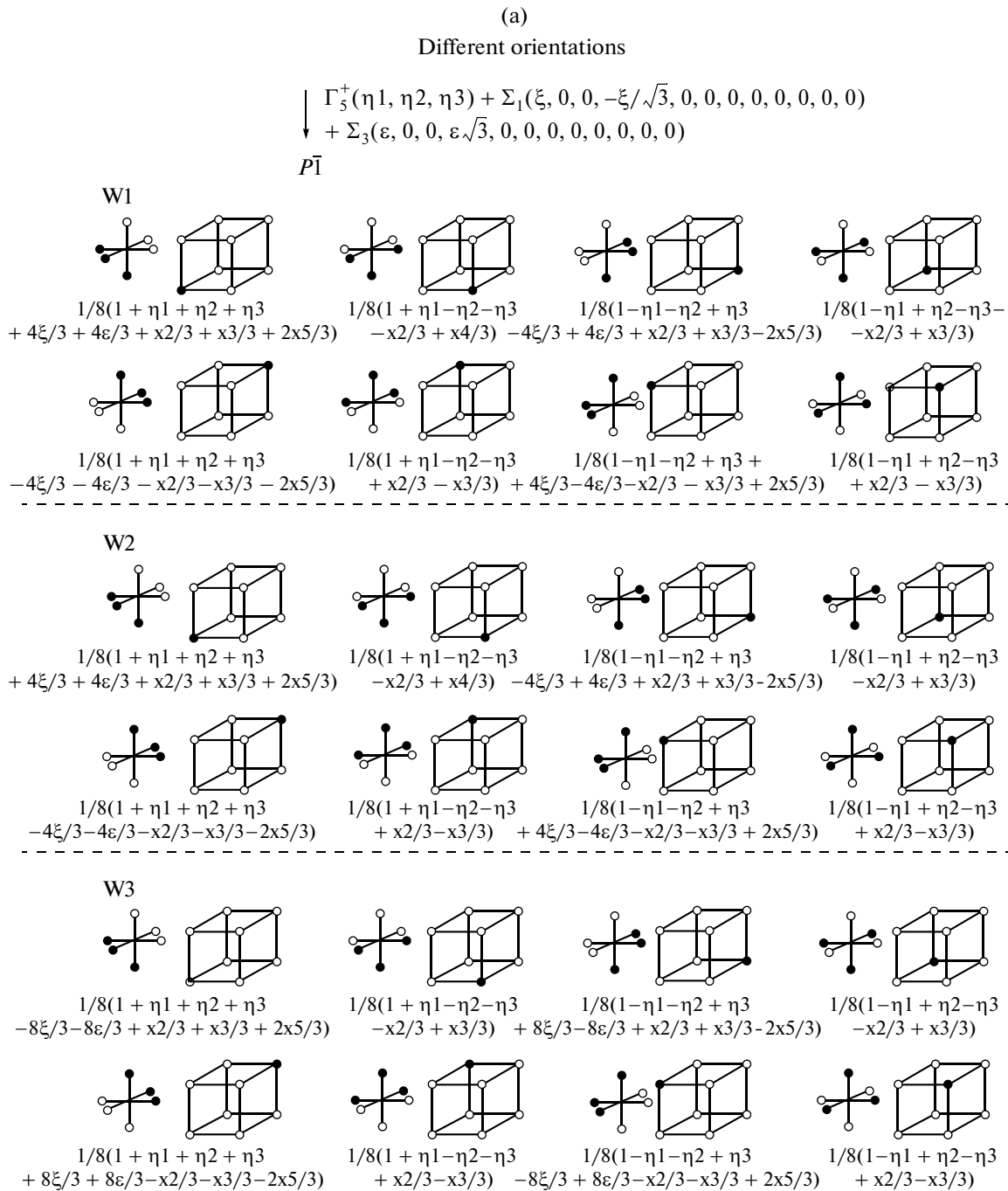


Fig. 7. Model of the ordering of the WO_3F_3 polyhedra in the C_{3v} configuration (see Fig. 1). Numbers under the particular orientation of the polyhedron indicate the probability of its existence; η_1 , η_2 , and η_3 are the components of the critical order parameter, which is transformed according to the Γ_5^+ representation; ξ is the component of the critical order parameter, which is transformed according to the Σ_1 representation; ε is the component of the critical order parameter, which is transformed according to the Σ_3 representation; and x_2 , x_3 , and x_5 are the components of the noncritical order parameters, which are transformed according to the X_2^- , X_3^- , and X_5^- representations, respectively.

entropy of this phase transition is equal to $R\ln 4$. Hence, the entropy of the phase transition associated with the ordering of the WO_3F_3 ion with invoking the

other critical order parameters of the representations Σ_1 and Σ_3 will be equal to $R\ln 8.8 - R\ln 4 = R\ln 2.2$; i.e., it will be almost two times smaller than $R\ln 4$.

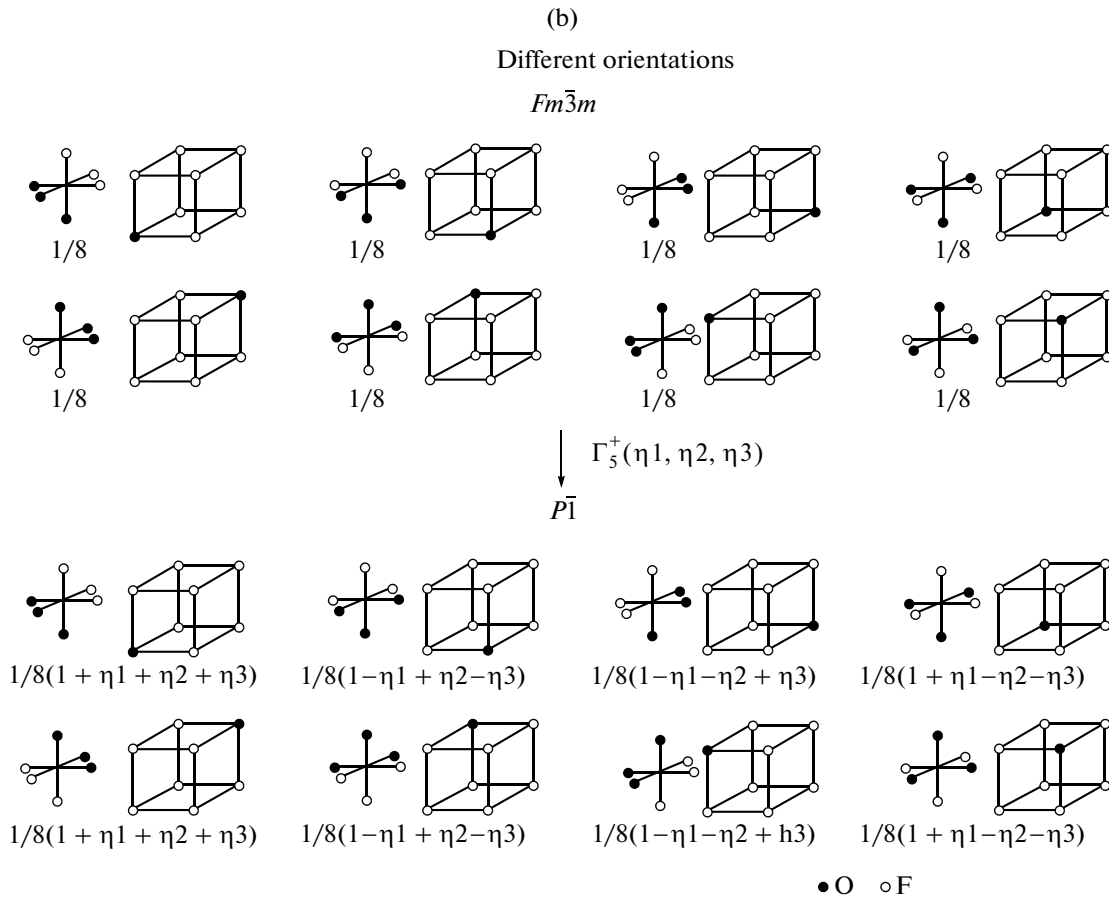


Fig. 7. (Contd.)

Thus, when the temperature decreases, the first phase transition is associated with the appearance of the order parameter that is transformed according to the representation Γ_5^+ . In the second phase transition, there appear the other two order parameters, which are related to the representations Σ_1 and Σ_3 . From the above reasoning, we can determine the symmetry of the intermediate phase G_1 . Table 4 presents the relationships between the components of the phenomenological order parameter, information about the symmetry of the phases of the $(\text{NH}_4)_3\text{WO}_3\text{F}_3$ compound, and the relationships between the basic translations of the unit cells of the parent cubic and distorted phases.

Continuing our consideration of the ordering of the WO_3F_3 polyhedron, in the third phase transition with the appearance of the order parameters $(\xi, 0, 0, -\xi/\sqrt{3}, 0, 0, 0, 0, 0, 0, 0, 0)$ of the representation Σ_1 and $(\varepsilon, 0, 0, \varepsilon\sqrt{3}, 0, 0, 0, 0, 0, 0, 0, 0)$ of the representation Σ_3 , we obtain the picture shown in Figs. 7 and 8, from which it can be seen that the aforementioned critical order parameters do not provide a complete ordering of the WO_3F_3 polyhedron in the triclinic

phase. However, the structure of this phase suggests that all WO_3F_3 polyhedra are completely ordered.

Now, it is appropriate to note that, in a number of cases, the distortion of the structure of the parent phase cannot be described only by the critical order parameters. In the distorted (disymmetric) phase, there can occur atomic displacements or atomic orderings that are compatible with the symmetry of this phase and which are specified by the noncritical (secondary) order parameters and irreducible representations. The entire set of order parameters, both critical and noncritical, which appear during the phase transition, forms the complete order parameter condensate [17].

The noncritical distortions have a secondary character and are insignificant in the vicinity of the phase transition points. The symmetry analysis indicates only the presence and type of noncritical order parameters. The numerical values of both the critical and noncritical distortions and order parameters involved in the complete condensate are determined from the experimental and, primarily, structural data.

Apart from the critical order parameters (the representations $\Gamma_5^+(11-7)$, $\Sigma_1(4-1)$, and $\Sigma_3(4-3)$), the

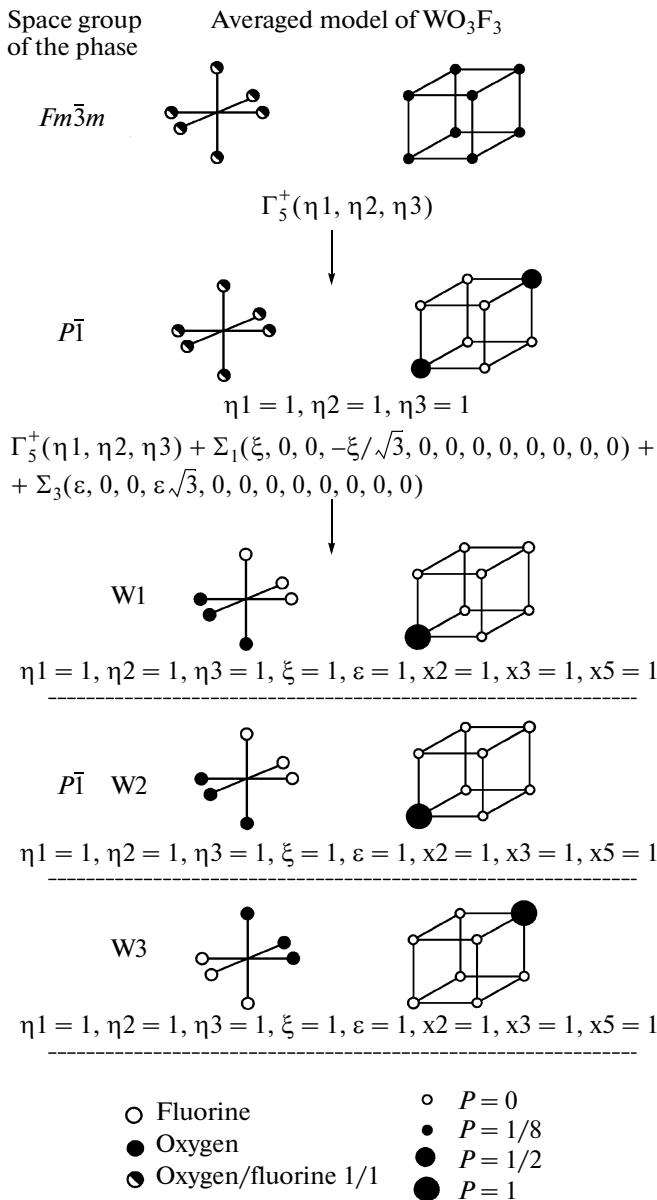
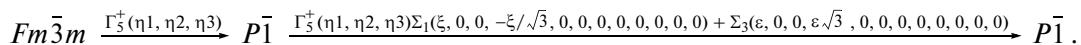


Fig. 8. Model and the shape of the WO_3F_3 polyhedron after averaging over all orientations for the maximum values of the critical and noncritical order parameters.

noncritical order parameters (the representations Σ_2 , Σ_4 , X_2^- , X_3^- , and X_5^-) are also involved in the process of ordering of the WO_3F_3 polyhedron and make an additional contribution to this ordering. The most noticeable contribution comes from the noncritical order parameters (the representations X_2^- , X_3^- , and X_5^-), so that their action leads to a complete ordering of WO_3F_3 (Figs. 7 and 8), which corresponds to that



obtained in the experiment. It should be noted that the total entropy of the ordering of this structural element is equal to $R\ln 8$.

We could not trace the behavior of the ammonium ions disordered in the cubic phase during the phase transitions because of the lack of information about the coordinates of hydrogen atoms in the distorted phase. However, since the entropy of the complete ordering of the WO_3F_3 polyhedron is equal to $R\ln 8$, i.e., it is close to the experimentally measured value $R\ln 8.8$, we can state that the ammonium ions are not ordered in the course of successive phase transitions. This is also indicated by the spectroscopy data reported in [8].

The process of ordering is accompanied by the displacements of the atoms W, N1, and N2 with respect to their positions in the cubic unit cell (Table 5). The position of the W atom is split into three positions W1, W2, and W3, and their displacements occur predominantly along the cubic axes **b** and **c**, which are controlled by the order parameters transformed according to the representations Σ_3 and Σ_1 , respectively. The remaining displacements of these atoms are small compared to those mentioned above and take place under the action of the noncritical representations Σ_2 , X_3^- , and X_5^- . The position of the N1 atom is split into three positions (N11, N12, and N13), and their displacements occur predominantly along the cubic axes **b** and **c**, which are controlled by the order parameters transformed according to the representations Σ_3 and Σ_1 , respectively. The remaining displacements of these atoms are small compared to those mentioned above and take place under the action of the noncritical representations Σ_2 and X_5^- . The position of the N2 atom is split into six positions (N21, N22, N23, N24, N25, and N26), and their displacements occur predominantly along the cubic axes **b** and **c**, which are controlled by the order parameters transformed according to the representations Σ_3 and Σ_1 , respectively. The critical representation Γ_5^+ also makes a significant contribution to the atomic displacements. Additional displacements are provided by the noncritical representations Σ_2 , Σ_4 , X_2^- and X_5^- .

5. CONCLUSIONS

Thus, using X-ray powder diffraction in combination with the appropriate procedures of the symmetry analysis of the complete order parameter condensate, we have determined the structural transformations occurring in the $(\text{NH}_4)_3\text{WO}_3\text{F}_3$ crystal, which can be schematically represented in the following form:

Table 5. Displacements of the W and N atoms in the G_2 phase with respect to their positions in the cubic unit cell

Atom	$\Delta x, \text{Å}$	$\Delta y, \text{Å}$	$\Delta z, \text{Å}$	$\Delta r, \text{Å}$
W1	0.005	0.040	0.062	0.073
W2	0.068	0.089	0.037	0.116
W3	0.066	0.075	0.014	0.100
N11	0.391	1.035	0.126	1.114
N12	0.104	0.149	0.225	0.290
N13	0.072	0.046	0.171	0.191
N21	0.080	0.133	0.045	0.154
N22	0.243	0.199	0.534	0.619
N23	0.024	0.248	0.516	0.573
N24	0.070	0.521	0.058	0.529
N25	0.054	0.069	0.087	0.123
N26	0.224	0.128	0.743	0.787

Here, the designations above the arrows refer to the critical representations and order parameters, which lead to this sequence of symmetry changes and are transformed according to the aforementioned representations.

The leading critical changes observed during the first phase transition in the structure under investigation are the ordering of the WO_3F_3 polyhedron and the displacement of the N2 atom, which is related to the critical order parameter (η_1, η_2, η_3) of the representation $11-7 (\Gamma_5^+)$. In this case, the entropy of the phase transition is equal to $R\ln 4$. The leading critical changes observed during the second phase transition in the structure are the further ordering of the WO_3F_3 polyhedron and the displacement of the N1 and N2 atoms along the cubic axes **b** and **c**, which are related to the critical order parameters ($\xi, 0, 0, -\xi/\sqrt{3}, 0, 0, 0, 0, 0, 0, 0, 0$) of the representation Σ_1 and ($\varepsilon, 0, 0, \varepsilon\sqrt{3}, 0, 0, 0, 0, 0, 0, 0, 0$) of the representation Σ_3 . The symmetry analysis of the structures of the phases G_0 and G_2 has demonstrated that the complete ordering of the WO_3F_3 polyhedra can be achieved only by the joint interaction of the critical parameters of the representations Γ_5^+, Σ_1 , and Σ_3 and the noncritical parameters $X_2^-, X_3^-,$ and X_5^- . The total entropy of the phase transitions in this case is equal to $R\ln 8$ and close to the experimentally observed entropy $R\ln 8.8$. During the phase transitions, the ordering of the ammonium ion does not occur.

ACKNOWLEDGMENTS

This study was supported by the Russian Foundation for Basic Research (project no. 09-02-00062) and the Council on Grants from the President of the Russian Federation for Support of Leading Scientific Schools of the Russian Federation (grant no. NSh-4645.2010.2).

REFERENCES

1. I. N. Flerov, M. V. Gorev, K. S. Aleksandrov, A. Tresaud, J. Grannec, and M. Couzi, *Mater. Sci. Eng.*, **R 24** (3), 81 (1998).
2. J. Ravez, G. Peraudeau, H. Arend, S. C. Abrahams, and P. Hagenmuller, *Ferroelectrics* **26**, 767 (1980).
3. M. S. Molokeev, S. V. Misyul', V. D. Fokina, A. G. Kocharova, and K. S. Aleksandrov, *Phys. Solid State* **53** (4), 834 (2011).
4. K. S. Aleksandrov, S. V. Misyul, M. S. Molokeev, and V. N. Voronov, *Phys. Solid State* **51** (12), 2505 (2009).
5. A. A. Udovenko, N. M. Laptash, and L. C. Maslennikova, *J. Fluorine Chem.* **124**, 5, (2003).
6. M. S. Molokeev and S. V. Misyul', *Phys. Solid State* **53** (8), 1672 (2011).
7. I. N. Flerov, M. V. Gorev, V. D. Fokina, A. F. Bovina, N. M. Laptash, *Phys. Solid State* **46** (5), 915 (2004).
8. A. N. Vtyurin, A. S. Krylov, Yu. V. Gerasimova, V. D. Fokina, N. M. Laptash, and E. I. Voit, *Phys. Solid State* **48** (6), 1067 (2006).
9. V. I. Mikheev, *X-Ray Determinant of Minerals* (Geologiya i Okhrana Nedr, Moscow, 1957) [in Russian].
10. J. W. Visser, *J. Appl. Crystallogr.* **2**, 89 (1969).
11. L. A. Solovyov, *J. Appl. Crystallogr.* **37**, 743 (2004).
12. K. S. Aleksandrov, S. V. Misyul, and E. E. Baturinets, *Ferroelectrics* **354**, 60 (2007).
13. H. T. Stokes, D. M. Hatch, and B. J. Campbell, *ISOTROPY: A Program Which Displays Information About Space Groups, Irreducible Representations, Isotropy Subgroups, and Phase Transitions* (Brigham Young University, Provo, Utah, United States, 2007); stokes.bue.edu/isotropy.html.
14. B. J. Campbell, H. T. Stokes, D. E. Tanner, and D. M. Hatch, *J. Appl. Crystallogr.* **39**, 607 (2006).
15. Yu. A. Izyumov and V. N. Syromyatnikov, *Phase Transitions and Crystal Symmetry* (Nauka, Moscow, 1984; Kluwer, New York, 1990).
16. O. V. Kovalev, *Irreducible and Induced Representations and Co-Representations of Fedorov's Groups* (Nauka, Moscow, 1986) [in Russian].
17. V. P. Sakhnenko, V. M. Talanov, and G. M. Chechin, *Fiz. Met. Metalloved.* **62** (5), 847 (1986).
18. E. I. Voit, A. V. Voit, A. A. Mashkovskii, N. M. Laptash, and V. Ya. Kavun, *J. Struct. Chem.* **47** (4), 642 (2006).

Translated by O. Borovik-Romanova